Influence of the morphology of InP substrates on interface roughness and defect density of quantum-cascade laser heterostructures

© D.S. Papylev[1], I.I. Novikov[1,2], V.V. Andryushkin[1,2], A.G. Gladyshev[2], V.V. Dudelev[3], L.Ya. Karachinsky[1,2], A.V. Babichev[1], I.A. Nyapshaev[3], A.Yu. Egorov[2,3], G.S. Sokolovskii[3]

[1] ITMO University,
197101 St. Petersburg, Russia
[2] Connector Optics LLC,
194292 St. Petersburg, Russia
[3] Ioffe Institute,
194021 St. Petersburg, Russia
E-mail: dspapylev@itmo.ru

Received September 18, 2025
Revised October 23, 2025
Accepted November 5, 2025

The influence of InP substrate of different manufactures on the structural properties of quantum-cascade laser heterostructures produced by molecular-beam epitaxy on metalorganic chemical vapor deposition templates was studied. A reduction in the root mean square interface roughness by 42−47 % as well as a decrease in surface defect density by a factor of 1.5−4.0 were demonstrated by using one type of substrate despite equal nominal substrate characteristics. The results confirm the critical importance the initial substrate quality in reducing the density of point defects and the roughness of the interfaces of quantum cascade lasers heterostructures.

Keywords: Quantum-cascade laser, interface roughness, defects, X-ray reflectometry, heterostructure.

DOI: 10.61011/SC.2025.07.62476.8580

1. Introduction

Heterostructures with InGaAs/InAlAs superlattices on InP substrates are the basis for the creation of quantum cascade lasers (QCL) in the mid-IR range [1–3]. In such superlattices containing layers with a thickness of several monolayers, the deviation of the actual thicknesses of the layers from the nominal ones and the imperfection of the interfaces can significantly affect the parameters of the laser [4]. In particular, the roughness of the interfaces of the heterostructure is the cause of elastic electron scattering, which causes parasitic energy transitions of electrons. As a result, these processes generate leakage currents and affect the occupancy of the upper radiative levels [5,6]. In addition, the roughness of the interfaces can affect the probability of resonant electron tunneling, thereby hindering the efficient transport of charge carriers [7]. Thus, the roughness of the heterostructure interfaces significantly affects the quantum efficiency and the threshold current QCL [8,9].

It is known that during epitaxy of heterostructures, the presence of initial defects on the substrate surface affects the structural quality of the grown epitaxial layers [10]. Despite the fact that the formation of a buffer layer of a heterostructure by metalorganic vapour phase epitaxy (MOVPE) potentially improves the morphology of the surface [11], the effect of the initial InP substrates on the structural quality of the QCL superlattice has not been sufficiently studied. The influence of the choice of substrates on the roughness of interfaces and the density of point defects in the heterostructure is studied in this paper.

2. Materials and methods

This paper studied quality of the interfaces of test QCL heterostructures grown using doped n^+ InP (100) substrates with a diameter of 2″ (two inches) from two different manufacturers, hereinafter referred to as P1 (manufactured in China) and P2 (manufactured in the USA). The substrates of both types have nominally identical characteristics according to the manufacturers' specifications. Before epitaxy of the QCL superlattices using P1 and P2 substrates, T1 and T2 templates were made, respectively. For this purpose, the substrates were grown with an InP layer with a thickness of 5000 nm using the MOVPE method in separate technological processes. Test heterostructures of QCL S1 (template P1) and S2 (template P2) were grown on the fabricated templates by molecular beam epitaxy (MBE) in two consecutive technological processes. The design of the heterostructure consisted of an InP substrate grown by the MOVPE method, an InP lining layer with a thickness of 5000 nm, a buffer layer of n-$In_{0.53}Ga_{0.47}As$ with a thickness of 50 nm and 10 cascades of superlattice of $In_{0.53}Ga_{0.47}As/In_{0.65}Ga_{0.35}As/In_{0.37}Al_{0.63}As$ with thickness of 2.7/*2.1*/0.9/3.2/ *2.6*/0.9/3.0/*2.1*/1.7/2.4/*1.5*/1.5/2.2/*1.5*/1.5/2.0/*1.3*/1.6/1.8/*1.3*/1.7/*2.8*/1.9/*2.8*/2.4/*2.8* nm with a total thickness of 52.2 nm. The final layer of the heterostructure was a 5 nm thick n-$In_{0.53}Ga_{0.47}As$ layer.

A common method for analyzing heterostructure parameters is X-ray diffractometry, which makes it possible to estimate the composition of epitaxial layers of the QCL heterostructure and determine the thickness of cascades of the QCL heterostructure with an accuracy of ~ 1 nm.

However, it is difficult to estimate the roughness of the heterostructure interfaces from X-ray diffraction curves. In this regard, the method of X-ray reflectometry was used to study heterostructures [12], a distinctive feature of which is a higher sensitivity to the thickness and roughness of the interfaces, as well as low sensitivity to the composition of the layers.

The heterostructures were studied using a high-resolution PANalytical X'Pert PRO MRD diffractometer with a hybrid four-crystal slit Ge (400) monochromator, and CuKα-1 radiation. X-ray reflectometry measurements were performed in the $2\Theta/\omega$-scanning mode in the angular range of $0-7.2^\circ$ with a step of 0.005°. The divergence of the X-ray beam is limited by the slits $(1/32^\circ)$ and $(1/16^\circ)$ for primary and reflected radiation, respectively.

Additionally, the surface of the heterostructures was studied by optical flaw detection on a KLA-Tencor Surfscan 6200 installation equipped with a laser with an operating wavelength of 488 nm. The measurements were carried out in two ranges of detection of point defects, determined by the gain on the photomultiplier. The ranges of the equivalent defect cross-sectional area were 0.6–10 and $10-250\,\mu m^2$. The surface roughness in the optical flaw detection method was characterized by the parameter $haze$, expressed in fractions of the intensity of scattered radiation to the intensity of laser radiation. The ratio between the value $haze$ and the RMS value of the surface roughness of the plate σ_{optic} was determined in accordance with the expression [13]:

$$haze = \left(4 \cdot \pi \cdot \cos(\theta_i)/\lambda\right)^2 \cdot R_0 \cdot \sigma^2_{\text{optic}}, \qquad (1)$$

where θ_i is the angle of incidence of the laser radiation on the surface, λ is the wavelength of the radiation, R_0 is the reflection coefficient of the surface.

3. Results

The measured X-ray reflectometry curves of test heterostructures S1 and S2 are shown in Figure 1. When comparing the results, the obtained curves are aligned according to the position of the critical angle of total external reflection. In this case, the indicative characteristics of roughness are the rate of intensity decrease near the critical angle, determined by the roughness of the surface of the upper layer, and the intensity of the peaks of oscillations, determined by the roughness of the interfaces. A qualitative comparison of the X-ray reflectometry curves makes it possible to judge a slightly higher surface roughness of the S1 heterostructure grown on a P1 substrate. More significant differences, characterizing the relatively large roughness of the S1 heterostructure, are observed in the intensity of the oscillation peaks, especially noticeable at large scanning angles, as shown in the inset of Figure 1.

The Fourier transform of the reflectometry curve [14] was used primarily to determine the thickness of the cascades of heterostructures, the results of which are displayed

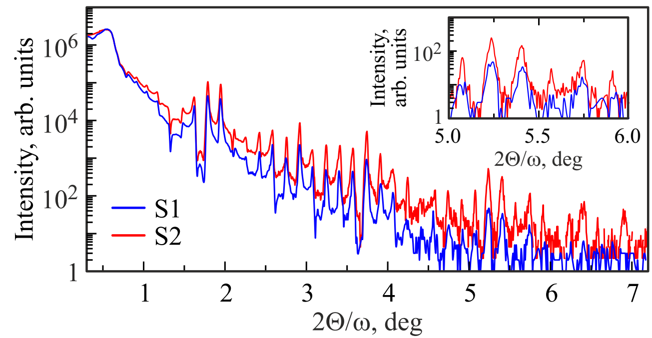

Figure 1. Results of measurement of X-ray reflectometry of heterostructures S1 and S2. The insert shows an enlarged fragment of the graph at large scanning angles.

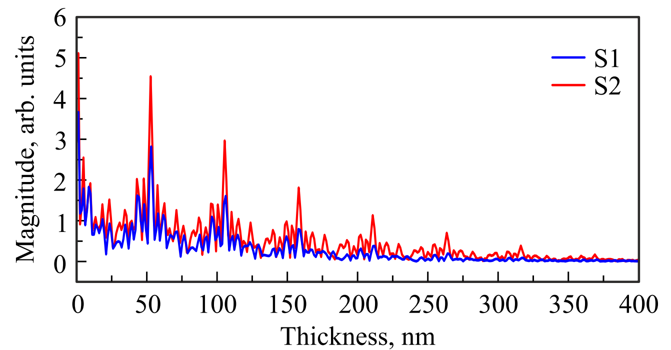

Figure 2. Results of the Fourier transform of the X-ray reflectometry curve of heterostructures S1 and S2.

depending on the depth in Figure 2. According to the observed Fourier images, quite pronounced peaks can be traced up to a thickness of ~ 300 nm. The inaccessibility for analysis of a larger thickness is due, on the one hand, to the low intensity of radiation reflection from deep-lying interfaces, and, on the other hand, to the angular scanning step during measurement. Thus, the X-ray reflectometry method allows analyzing the parameters of the upper cascades, while using the X-ray diffractometry method, it is possible to study the entire thickness of the heterostructure. According to the position of the peaks observed in Figure 2 equidistant from each other, it is possible to judge the high accuracy of reproducing the thickness of the cascades. The cascade thicknesses calculated from the most intense peak of the Fourier image were 52.7 and 52.8 nm, which correspond to deviations from the nominal values by 0.5 and 0.6 nm for heterostructures S1 and S2, respectively.

To quantify the roughness of the heterostructure interfaces, X-ray reflectometry curves were modeled based on the Paratt equations [15,16]. The intensity of reflected radiation X_j from the interface of the layer j is described by the recursive formula:

$$X_j = \left(\exp\frac{-i\pi R_{j+1}t_{j+1}}{\lambda}\right)^4 \cdot \frac{X_{j-1} + R_{j+1}}{1 + X_{j-1}R_{j+1}}; \qquad (2)$$

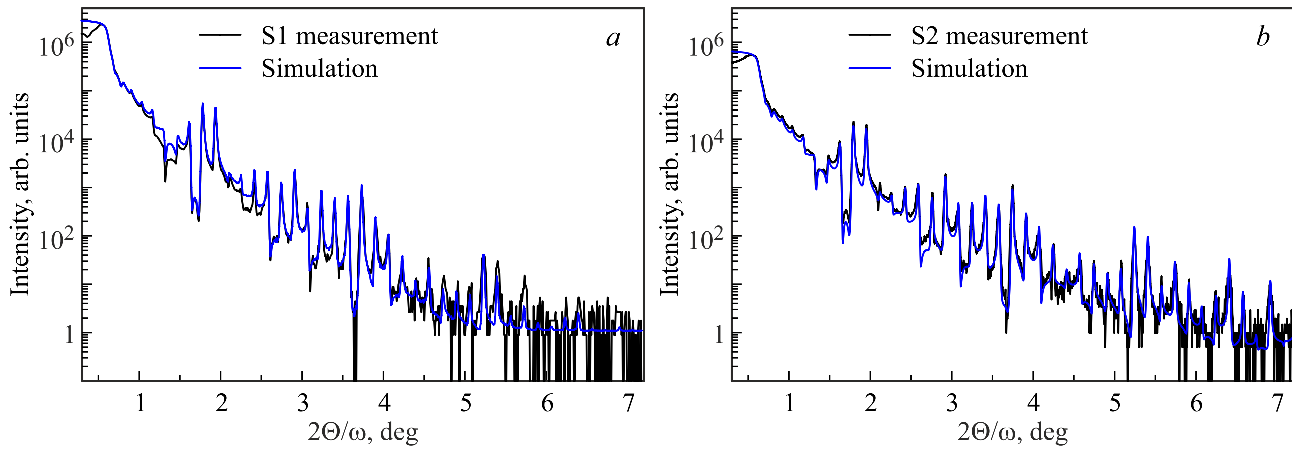

Figure 3. Simulation results of the X-ray reflectometry curve of heterostructures S1 (*a*) and S2 (*b*).

$$R_j = \frac{r_j - r_{j+1}}{r_j + r_{j+1}} \exp(-2r_j r_{j+1} \sigma_{j+1}); \quad (3)$$

$$r_j = \sqrt{\omega^2 - 2\delta_j - i2\beta_j}, \quad (4)$$

where R_j is the reflection coefficient, t is the thickness, ω is the angle of incidence, δ and β are components of the complex refractive index of the layer, σ_{j+1} is the RMS value of the roughness of the interface of the layer with an index of $j+1$. During the modeling, the thicknesses and roughness of the layers were selected to ensure the best match between the experimental and simulated curves. The mean square roughness σ_{int} was assumed for all interfaces of the heterostructure. The RMS surface roughness of the σ_{surf} heterostructure was selected independently of σ_{int}. The results of modeling X-ray reflectometry curves are shown in Figure 3.

The parameters determined as a result of modeling the reflectometry curves are presented in Table 1. The results obtained demonstrate a significant 1.7–1.9-fold decrease in the root-mean-square roughness of the surface and interfaces of the heterostructure when using a substrate P2.

The thicknesses of the superlattice cascades determined by modeling and Fourier transformation methods show that there are no significant differences between the heterostructures S1 and S2. The values obtained are in the range of thickness errors determined by the position of thickness oscillations on the X-ray diffractometry curve (52.3 ± 1.0 nm and 52.5 ± 0.9 nm for S1 and S2, respectively). When comparing the measurement results, X-ray reflectometry should be considered as a more accurate method for determining the thickness of the cascades of the QCL heterostructure, taking into account the maximum depth available for analysis, not exceeding 300 nm.

According to the measurement results by optical flaw detection method presented in Table 2, both substrates P1 and P2 are characterized by a low density of point surface defects. At the same time, the substrate P1 has a higher surface roughness compared to the substrate P2. An analysis

Table 1. Roughness and thickness parameters determined by modeling the reflectometry curve of heterostructures S1 and S2

Sample	σ_{int}, nm	σ_{surf}, nm	Thickness of cascade, nm
S1(P1)	0.55	0.59	52.7 ± 0.1
S2(P2)	0.32	0.31	52.7 ± 0.1

of the surface of the templates showed a slight increase in the initial density of point defects and roughness as a result of high-temperature substrate overgrowth. The obtained measurement results are typical for a series of similar substrates and templates manufactured in various (more than three) growth processes. When studying the heterostructures, it was revealed that the sample S2 is characterized by a ~ 1.5-fold lower density of point defects in the measurement range of $10-250\,\mu\text{m}^2$ and more than 4-fold lower density of defects in the measurement range of $0.6-10\,\mu\text{m}^2$ compared with the sample S1.

When analyzing the roughness of heterostructures S1 and S2, there are no significant differences detected by X-ray reflectometry. The reason for the observed discrepancy may be the uneven distribution of surface roughness over the area of the heterostructure. As can be seen from the density distribution maps of point defects shown in Figure 4, the highest value of *haze* is observed near the edges of the heterostructure. However, when measured by X-ray reflectometry, the X-ray beam is directed to the center of the plate. At small scanning angles, near the critical angle of total reflection, the length of the irradiation area can be ~ 10 mm. Therefore, for a more correct comparison of the results, the central regions of plates with a size of 10×10 mm were studied using optical flaw detection. The measurement results are summarized in Table 3, and maps of defect density distributions in the central region of heterostructures are shown in Figure 4. It is determined

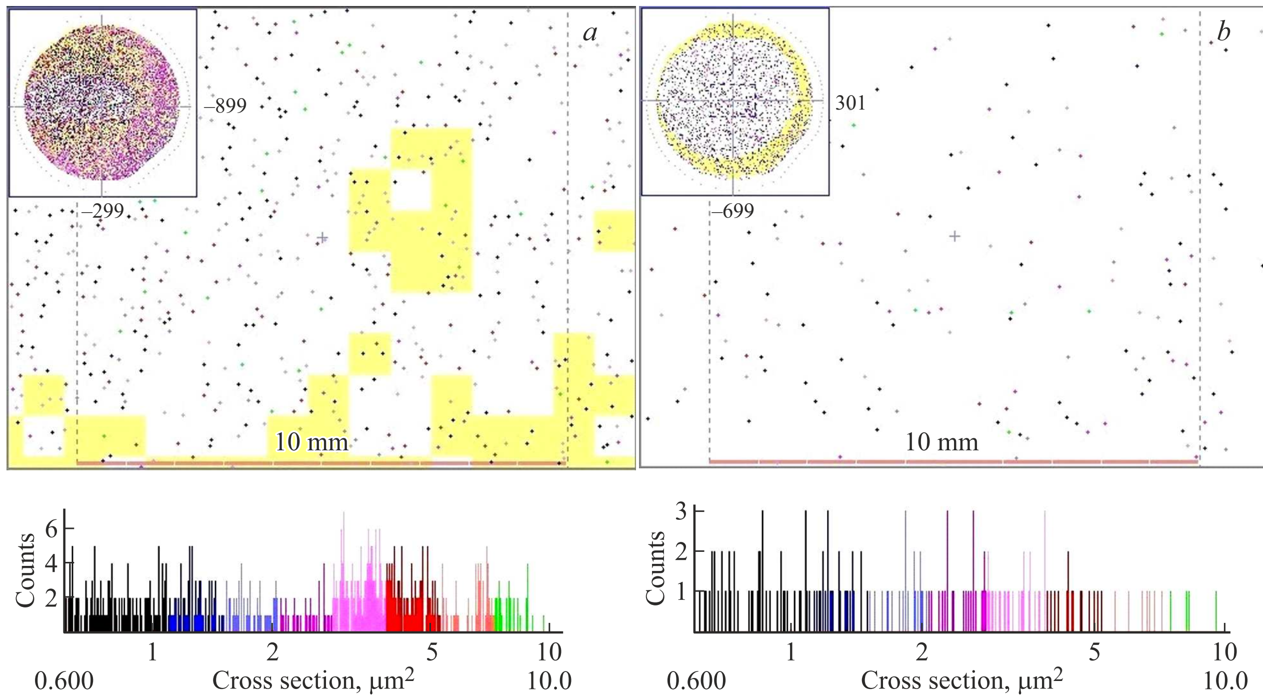

Figure 4. Map of surface defects in the central region of the test heterostructure S1 (*a*) and S2 (*b*) in the measurement range of $0.6-10\,\mu m^2$.

Table 2. Density of point defects and surface roughness of samples determined by optical flaw detection

Sample	Range $0.6-10\,\mu m^2$			Range $10-250\,\mu m^2$		
	Density of defects, units/cm^2	*haze*, ppm, mln^{-1}	σ_{optic}, nm	Density of defects, units/cm^2	*haze*, ppm, mln^{-1}	σ_{optic}, nm
P1	0.063	38.8	0.42	0.063	18.80	0.30
P2	1.57	6.74	0.18	1.19	1.09	0.07
T1(P1)	1.89	40.6	0.43	0.377	19.6	0.30
T2(P2)	1.95	7.18	0.18	2.33	1.36	0.08
S1(P1)	549	94.0	0.56	9.12	63.2	0.46
S2(P2)	126	86.6	0.53	6.54	62.6	0.45

Table 3. Density of point defects and surface roughness in the central region of heterostructures S1 and S2

Sample	Range 0.6–10 um^2			Range $10-250\,\mu m^2$		
	Density of defects, units/cm^2	*haze*, ppm, mln^{-1}	σ_{optic}, nm	Density of defects, units/cm^2	*haze*, ppm, mln^{-1}	σ_{optic}, nm
S1(P1)	519	44	0.38	7.56	0	0
S2(P2)	143	12.3	0.20	9.24	0	0

that the density of point surface defects in the central part of the heterostructures is approximately equal to the corresponding value over the entire plate area. The study of the parameter *haze* in the central part of the plate showed the absence of roughness, fixed in the range of $10-250\,\mu m^2$. When measured in the range of $0.6-10\,\mu m^2$, the RMS roughness was estimated at 0.38 and 0.20 nm for heterostructures S1 and S2, respectively. Despite the fact that the absolute values of the RMS roughness obtained by optical flaw detection are slightly lower than those determined by X-ray reflectometry, the relative difference between samples S1 and S2 is about 2 times and correlates with the results obtained by X-ray reflectometry. As a result, the optical flaw detection method can be used to assess the

surface roughness of a heterostructure. Nevertheless, when comparing the results with X-ray reflectometry data, the uneven distribution of roughness over the plate should be taken into account.

The noted effect of substrate quality on the defect density and the roughness of superlattice interfaces was confirmed by the analysis of heterostructures S3 and S4 by optical flaw detection. The heterostructures were grown on templates similar to T1 and T2, respectively. The superlattices of the heterostructures consisted of 10 cascades of $In_{0.65}Ga_{0.35}As/In_{0.37}Al_{0.63}As$ with thickness of *3.6*/1.4/*3.8*/1.3/*4.3*/1.3/*1.2*/3.8/*1.8*/2.7/*1.8*/2.1/*2.0*/2.1/*2.1*/1.9/*2.2*/1.8/*2.5*/1.7/*2.8*/2.2 nm. Unlike samples S1 and S2, the heterostructures were grown by the MPE method in a single epitaxial process. The density of point defects of the S4 heterostructure is determined to be 2.6−6.9 times less, and the RMS roughness is 56 % lower than RMS roughness of the heterostructure S3. The roughness and density of defects similar to the sample S3 were obtained by sequential epitaxy of two similar heterostructures S3.

Thus, it was shown that the bonding of substrates by the MOVPE method with an InP layer with a thickness of 5000 nm does not provide complete planarization of the epitaxial surface. As a result, the roughness of the interfaces of the active region of the QCL is largely determined by the initial roughness of the substrate. When studying the quality of the heterostructure interfaces by X-ray reflectometry, it was found that the use of the substrate P2 leads to a decrease in the root-mean-square surface roughness of the heterostructure by 1.7−1.9 times compared with the substrate P1. The RMS roughness of the heterostructure interfaces on the substrate P2 was ~ 0.3 nm. Optical flaw detection measurements also confirmed a lower surface roughness of the heterostructure grown on the substrate P2 and showed a decrease in the density of point defects by 1.5−4.0 times compared with the heterostructure grown on the substrate P1.

Funding

The study was conducted at the expense of a grant from the Russian Science Foundation No. 21-72-30020-P, https://rscf.ru/project/21-72-30020/

Conflict of interest

The authors declare that they have no conflict of interest.

References

[1] A.Yu. Egorov, A.V. Babichev, L.Yu. Karachinsky, I.I. Novikov, E.V. Nikitina, M. Tchernycheva, I.S. Tarasov. Semiconductors, **49** (11), 1527 (2015).
[2] A.V. Babichev, A. Bousseksou, N.A. Pikhtin, I.S. Tarasov, E.V. Nikitina, A.N. Sofronov, A.Yu. Egorov. Semiconductors, **50** (10), 1299 (2016).
[3] A.V. Babichev, A.S. Kurochkin, E.S. Kolodeznyi, A.V. Filimonov, A.A. Usikova, V.N. Nevedomsky, A.Yu. Egorov. Semiconductors, **52** (6), 745 (2018).
[4] Y. Zhao, J. Zhang, C. Cai, J. Chen, X. Zhao, C. Liang, R. Che. ACS Appl. Mater. Interfaces, **12** (37), 41950 (2020).
[5] Y. Chiu, Y. Dikmelik, P.Q. Liu, N.L. Aung, J.B. Khurgin, C.F. Gmachl. Appl. Phys. Lett., **101** (17), 171117 (2012).
[6] C. Boyle, K.M. Oresick, J.D. Kirch, Y.V. Flores, L.J. Mawst, D. Botez. Appl. Phys. Lett., **117** (5), 051103 (2020).
[7] J.B. Khurgin, Y. Dikmelik, P.Q. Liu, A.J. Hoffman, M.D. Escarra, K.J. Franz, C.F. Gmachl. Appl. Phys. Lett., **94** (9), 091101 (2009).
[8] Y.V. Flores, S.S. Kurlov, M. Elagin, M.P. Semtsiv, W.T. Masselink. Appl. Phys. Lett., **103** (16), 161102 (2013).
[9] K.A. Krivas, D.O. Winge, M. Franckié, A. Wacker. J. Appl. Phys., **118** (11), 114501 (2015).
[10] M. Adamcyk, T. Pinnington, A. Ballestad, T. Tiedje. Mater. Sci. Eng. B, **75** (2-3), 153 (2000).
[11] L. Cheng, J. Fan, D. Janssen, D. Guo, X. Chen, F.J. Towner, F.S. Choa. J. Electron. Mater., **41** (3), 506 (2012).
[12] E. Chason, T.M. Mayer. Crit. Rev. Solid State Mater. Sci., **22** (1), 1 (1997).
[13] A. Steinbach, U. Subramaniam. *Be market ready* (KLA-Tencor Corporation, 2006) v. 66.
[14] M. Lammel, K. Geishendorf, M.A. Choffel, D.M. Hamann, D.C. Johnson, K. Nielsch, A. Thomas. Appl. Phys. Lett., **117** (21), 213104 (2020).
[15] L.G. Parratt. Phys. Rev., **95** (2), 359 (1954).
[16] P.F. Fewster. Rep. Progr. Phys., **59**, 1339 (1996).

Translated by A.Akhtyamov